Bull. ERS, No.10 (1976)

EARTHQUAKE GROUND MOTION AT ROCKY GROUND INTERSPERSED WITH THIN SOFT LAYERS

by

C. Tamura[I], S. Okamoto[II] and H. Kawakami[III]

§1. Introduction

Since 1962, the authors have been carrying out earthquake observations at the surface and underground at rocky ground in a mountainous part of the Kanto Region 150 km north of Metropolitan Tokyo.

The observation site is located at Kinugawa Underground Power Station of Tokyo Electric Power Company. A portion of the results of observation has been previously reported [1]. In this present paper, the influence of thin clay layers interspersed in the rock on earthquake ground motion is mainly described.

It is clear that although the soft layers in the rock ground at this site are fairly thin the influence on earthquake ground motion is not small but significant.

§2. Outlines of Geology and Seismometers

The geology of the observation site consists of green tuff ranging from Tertiary to Quaternary, and is comparatively homogeneous. The geological condition at a bore hole at the site is shown in Table 1. Three clay layers produced by weathering of green tuff are interspersed in the rock at depths of about 16 m, 36 m and 47 m, while there are also some cracks at 50 m and 52 m.

As for a vertical shaft constructed for access to the underground power station and which is at a distance of 14 m from the bore hole, a clay layers exists between depths of 13.8 m and 14.25 m, and the top layer to 10 m or more in depth is comparatively weathered. Rock bolts were used at a depths between 33 m and 39 m during construction, while there was no core recovery between 53.4 m and 54.8 m.

The cross section of the vertical shaft is 5 m by 7 m and the depth is 67.2 m. Two displacement seismometers of natural period of 1 sec are set at the surface and at the bottom of the shaft, and 5 accelerometers, of natural period of 0.3 sec and having integrated frequency characteristics nearly flat in range of 0 to 24 Hz, are installed at the surface and at depths of 17.2 m, 34.2 m, 52.2 m and 67.2 m.

I) Professor, II) Professor Emeritus and III) Post Graduate Student; Institute of Industrial Science, University of Tokyo

In the bore hole, 8 accelerometers having integrated frequency characteristics nearly flat in range of 0 to 10 Hz are set and buried at depths of 9 m, 14 m, 16.5 m, 42 m, 50 m, 58 m and 67 m, taking the locations of the thin soft layers into consideration. Accordingly, there have been noticeable differences between acceleration waveforms recorded at the bore hole and those recorded at the vertical shaft (Fig. 1).

§3. Reports on Results of Earthquake Observations

Up to this time, more than 200 earthquakes have been recorded and some of them have been analyzed and the results previously published. An outline is given here of the results of analyses performed since them.

3.1 Direction of Travel of Earthquake Motion

It is well known that earthquake motion travels in the form of body waves and surface waves. In earthquake engineering, it is of importance to investigate how earthquake wave motions are propagated locally. Kanai et al., found from observations of nearby earthquakes that the properties of predominant vibration portions of surface layers are governed by phenomena of multiple reflection [2], while Aki et al., as a result of observing earthquake motions of nearby earthquakes from three points, discovered that secondary earthquake motions of comparatively slow propagation speeds are generated at the ground surface because of the existence of surface layers [3].

At the observation site of Kinugawa Underground Power Station, accelerations are being observed simultaneously at several points between the ground surface and approximately 67 m underground. The directions of advance of earthquake waves at the surface portion of the rocky ground were investigated based on acceleration waveforms obtained there. The speeds of feeding paper of the oscillographs for recording accelerations and displacements were approximately 10 cm per sec. Time lags in acceleration waveforms were determined by two methods.

One is that of taking out a period of approximately 4 sec from the major portion of earthquake motion, reading the waveforms at intervals of approximately 1/200 sec, computing cross-correlations, and determining the time lags between the waveform at the surface and the waveforms at various depths.

Fig. 2 is for the Off-Nemuro Peninsula Earthquake ($M = 7.4$, $\Delta = 870$ km) of June 17, 1973, and Fig. 3 for the earthquake ($M = 5.3$, $\Delta = 140$ km) of June 13, 1971 with abscissas indicating time lag and ordinates indicating depth. It may

be seen from these figures that time lag has a linear relation with depth.

The other is a method taking advantage of cases where several predominant peaks are clearly distinguished in acceleration waveforms to find the propagation conditions by measuring time lags of peaks in the acceleration waveforms according to depth. Fig. 4 shows the time lags obtained in this manner for the earthquake of November 12, 1974 (M = 4.9, Δ = 80 km). At this observation site, it may be considered that earthquake waves travel from under the ground toward the surface and are then reflected.

Next, time lags determined from cross-correlations indicated as functions of the directions of focuses are indicated in Fig. 5. The 0 on the abscissa is the angle formed by a line connecting the observation site to a focus and by the vertical direction. From this figure, it is seen that the direction of incidence to the ground surface is almost completely unrelated with the location of the focus.

Assuming next that the ground is an isotropic elastic body of Poisson's ratio of 0.25, the interrelations between earthquake waves at 67.2 m underground in case of incidence of SH waves or SV waves at a certain angle and waves at the ground surface were calculated (Fig. 6). The incident angles in this case were taken to be within the critical angle.

Concerning SH waves, since the direction of travel of reflected waves in case of incidence to a sloped surface differs from that in case of incidence to a horizontal surface, the time lags of reflected waves are shorter compared with the time lags of incident waves. And, when SV waves are incident, reflected SV waves and P waves are produced. P waves have a different direction of travel from reflected SV waves. Therefore, in this case, the form of cross-correlation of earthquake waveforms at the ground surface and at a point 67.2 m underground will be complex.

The form of cross-correlation in Fig. 6 shows that time lag of reflected waves and apparent reflection factor vary according to type of incident wave and direction of incidence. Considering that in analysis of earthquake waveforms time lags of reflected waves are more often shorter than time lags of incident waves, that reflection coefficients are from 1 to 0.5 with around 0.5 predominant, and that the gradient of the slope at the measurement point may be seen to be 18° to 20°, the results of these calculations can be said to explain the phenomena fairly well.

The propagation speed of earthquake waves (S waves) in the vertical direction at this particular site is 1.6 km/sec which is a slightly smaller figure than the propagation speed surmised from test results on the boring core. The reason

for this probably is that propagation at the surface layer portion is 1.6 km/sec and smaller than the S wave speed of approximately 3 km/sec of the so-called earth's crust.

3.2 Distribution of Acceleration Amplitude along Depth

The acceleration amplitudes obtained from power spectra of accelerations at various depths and plotted result in Fig. 7. The ordinate indicates depth. This figure shows that in the range of comparatively low frequencies, amplitudes are roughly constant regardless of depths and wave lengths becomes shorter with increase in frequency. There is good agreement with amplitude distribution for the case of a standing type wave of speed of 1.6 km/sec, reflection factor of 0.5 advancing up to the ground surface from below to be reflected at the surface and again travel downward. However, with a number of earthquake records, the amplitude distributions do not agree with such a distribution, and it was also found that the time lag relation described in 3.1 was not indicated.

Fig. 8 shows the amplitude distributions of such earthquakes. It may be seen that the amplitude distributions at low frequencies are completely different for the observation points Nos. 1, 4 and 5, and Nos. 2 and 3.

Fig. 9 gives the basic waveforms of accelerations recorded at the vertical shaft for the Niigata Earthquake ($M = 7.5$, $\Delta = 180$ km), one of this earthquake group. It is clearly seen that different vibrations from those at the No. 1, No. 4 and No. 5 observation points are predominant at No. 2 and No. 3.

§4. Influence of Condition of Surface Layer on Earthquake Motion

As described in §3, it was learned regarding distribution according to frequency of acceleration amplitudes in the direction of depth that it could be explained more or less by considering reflection at the ground surface of wave motion progressing upward from below. It was also found, however, that there were cases of distributions indicated which could not be explained by this reflection theory. The latter will be discussed here.

Concerning earthquake motion along the direction of depth in bedrock, Kanai, as a result of earthquake observations at depths of 150 m, 300 m and 450 m from the ground surface, found a distribution of displacement indicating a peak value at 150 m, and suggested that this might be the surface wave calculated by Sezawa.

As mentioned in §3, it has been clarified that earthquake wave motions at this observation site are propagated from below in a generally vertical direction, and accordingly, it may be considered that the phenomenon of amplification of amplitudes of S waves of the major portions of earthquakes seen at the surface layer is due to such propagation of earthquake wave motion. It is thus that may it be surmised the dynamic properties of the surface layer greatly influence the character of earthquake motion.

4.1 Ground Model

As a result of comparing the properties of the core recovered from the bore hole and the condition of the ground observed during excavation of the vertical shaft, it was found that the location was not necessarily of uniform stratification. Referring to the measurements of seismic wave velocities and density of soils carried out at the bore hole to investigate the dynamic properties of the surface layer portion, a model as shown in Fig. 10 was made.

The bottom part of the ground model (the part deeper than observation point No. 4 in the vertical shaft) is fairly hard and it may be surmised from waveforms observed that this part is almost completely unaffected by the surface layer portion. Since the purpose of the present study is to clarify the dynamic characteristics of the surface layer portion, it was decided that the ground model should be the portion shallower than observation point No. 4 in the vertical shaft, and the dynamic properties of this part were examined.

In this model, the maximum propagation speed of 200 m for S waves in clay strata was computed from the results of speed measurements at the bore hole, and correspond to propagation speeds in cases of microstrains. For other parts, the speeds were taken to be from 500 m/sec to 1,700 m/sec. These were determined based on the average propagation speed being of the order of 1,600 m or somewhat higher and in consideration of the condition of the ground. Densities were assumed to be 2.5 ton/m^3 at portions of rock and 2.0 ton/m^3 at clay. As indicated in Fig. 10, the model was divided into layers numbered 1 to 6 from the top, the No. 2 and No. 4 strata being clay layers. The propagation speeds of shear waves at the respective layers were taken to be v_1, v_2 ...., v_6.

4.2 Dynamic Characteristics of Ground Model

In analysis of this ground model the fact that the soil strata of this particular site are distinctly divided into hard rock portions and clay layers must be noted, and it is of extreme importance how the dynamic characteristic of the

clay layers — reliance on strain of rigidity of clay — is evaluated. Therefore, in this analysis, the properties of rock were considered to be constant, whereas for the clay layers, 200 m/sec was taken as the upper limit of propagation speed with various lesser speeds assumed, and the responses indicated by the ground model were accordingly investigated.

4.2.1 Natural Period and Natural Mode

The calculation conditions and natural frequencies are given in Table 2.

Fig. 11 shows the relation between the speed v_4 at layer No. 4 and fundamental vibration period T_1 with the speed v_2 of layer No. 2 as a parameter. According to this, it may be seen that when about 25 m/sec is taken for v_2, T_1 is constant practically without relation to v_4, while when v_4 is about 25 m/sec, T_1 is not influenced very much by v_2. It may further be seen that the effect of v_4 appears more prominently in T_1 as v_2 increases.

When the propagation speed at layer No. 2 or layer No. 4 is lowered to around 25 m, the two become practically independent of each other, and when the speeds at both are lowered, T_1 converges toward a constant value (about 1 sec). According to this ground model, it may be surmised that a natural vibration of around 1 Hz to around 3 Hz is produced by lowering of propagation speeds in layers No. 2 and No. 4.

Fig. 12 through 14 respectively show the fundamental and the second modes by solid lines and broken lines, respectively, for Case 2, Case 4 and Case 8. These mode diagrams indicate that when a natural vibration of the surface layer is induced extreme shear strains are produced in the clay layers.

4.2.2 Variation in Participation Factor According to Natural Frequency

The participation factors obtained for the modes in 4.2.1 are shown in Figs. 15 and 16. These figures indicate that when v_2 is 200 m/sec, the participation factor is 70% or higher irregardless of v_4, and when v_2 is lowered the participation factor is also lowered, while in case v_2 is decreased below 100 m/sec, the participation factor shows a trend of increase as v_4 is lowered. This means that with respect to the fundamental mode the participation factor is increased when v_4 is constant or is decreased.

In effect, when the fundamental vibration is produced, large strains are produced on layer No. 4 to result in reduction of v_4, by which participation factor increases, the fundamental period becomes longer, amplitude is increase, and

there is a trend for the fundamental vibration to become even more predominant.

4.2.3 Frequency Characteristics of Ground Model

Fig. 17 shows the frequency characteristics of this ground model when a standing sine wave motion of any frequency is incident from below and corresponds to Case 20. The solid line and the broken line in this figure are the frequency characteristics of the ground surface and the top of layer No. 3, respectively, for input of a unit amplitude.

From this figure, it may be seen that in the vicinities of the fundamental and the second natural frequencies of this ground model the respective vibration modes are predominant whereas at other parts smaller amplitudes are indicated compared with the amplitude of incident wave motion, and especially, with frequencies higher than secondary frequencies at around 10 Hz, this surface layer portion indicates vibration of smaller amplitude in comparison with incident waves. This explains well the characters of actual earthquake records as will be described later. These phenomena serve to show how great is the influence of the thin interspersed clay layers on the dynamic characteristics of the surface layer ground.

§5. Characteristics of Earthquake Motion

In §3 it was said that earthquake motion at the ground surface of this location could be explained in general by the theory of reflection at the surface of uniform ground. However, the earthquakes listed in Table 3 are cases in which dynamic characteristics of the surface layer which cannot be explained by this theory were seen. On examination of earthquake waveforms, it appears that the dynamic characteristics of the surface layer portion do not become conspicuous in cases of earthquakes of small magnitude and cases of low acceleration. Also, it appears the dynamic characteristics cannot be seen at the coda wave parts of earthquake motions.

5.1 Frequency Characteristics

Periods of waves appearing predominantly at only observation points at the surface portion (Nos. 1, 2 and 3 of vertical shaft of Fig. 1) and the number of occurrences as seen from comparisons of records made through the results of calculations of power spectra for the main parts of

acceleration records and through visual examinations are indicated in Fig. 18. The ordinate gives the number of occurrences when considering an earthquake as the unit. From this figure, it may be seen that in general the number of occurrences is large limited to the low-frequency part of 2 to 3 Hz. Especially, the number is large at around 3 Hz. It may also be seen there is predominance between 4 and 6 Hz, particularly, in the vicinity of 5 Hz. At 8 Hz and higher, there is no marked amplification at any specific frequency and the distribution appears to be over a wide frequency range.

The acceleration power spectra of the earthquakes of April 6, 1965 ($M = 5.5$, $\Delta = 88$ km) and September 18, 1965 ($M = 5.7$, $\Delta = 174$ km) are given in Figs. 19 and 20. Fig. 21 shows the power spectra of the records obtained at the vertical shaft at the time of the Niigata Earthquake. The feature of the records of this earthquake is that predominant vibrations with frequencies at around 1 Hz and around 1.6 Hz were produced at observation points Nos. 1 to 3. Moreover, these are most prominent at the major portions where accelerations indicate maximums. The amplitudes of displacement records also show maximum values at these parts. The modes of acceleration of the parts of 1 Hz and 1.6 Hz are indicated in Fig. 22.

5.2 Phase of Acceleration Waveform

Cross-correlograms calculated for the record at the ground surface and the record at each depth taking the main parts of acceleration during the Niigata Earthquake are given in Fig. 25. In this figure, it may be seen that unlike observation points No. 4 and No. 5, time lags from the ground surface cannot be seen distinctly for No. 2 and No. 3.

As a result of comparing the records of Nos. 1 to 5 regarding the main parts of waves of around 1 Hz, the following was found regarding time lags:

No. 1 and No. 2:	No. 2 lags by approximately 0.045 sec
No. 2 and No. 3:	Practically no time lag
No. 3 and No. 4:	No. 4 faster by 0.68 to 0.70 sec
No. 4 and No. 5:	Practically no time lag

The distance between observation points is approximately 17 m, and assuming the propagation speed of S waves to be 1,600 m/sec, there should have been a time lag of approximately 0.01 sec between observation points. Notwithstanding, in this case, No. 1, No. 2 and No. 3, and No. 4 and No. 5

comprised separate groups, and there were relatively great time lags between the respective groups. It may also be seen that geometric waveforms are extremely similar within each group. A similar phenomenon has been recognized in records obtained at the vertical shaft and bore hole in case of the earthquake (M = 5.8, Δ = 98 km) which occurred near the observation site on August 4, 1974.

§6. Consideration

As described in the foregoing, it has been clarified that the ground condition of the surface layer has a great effect on earthquake motion even at rocky ground. A discussion of strains in clay layers interspersed in bedrock will be made here.

Among earthquakes observed up to this time, the one of April 6, 1965 is a case other than the Niigata Earthquake in which displacement amplitude measured by displacement meter was large, acceleration was high, and in addition the dynamic characteristics of the surface layer was clearly noticeable. The magnitude of this earthquake was 5.5, epicentral distance 88 km, depth 60 km, while a maximum displacement of 335 μ was indicated at the ground surface and acceleration was a maximum of 48.9 gal at observation point No. 3 and 17.6 gal at No. 5. Fig. 19 gives the acceleration power spectra of this earthquake. In the case of this earthquake a very predominant vibration was seen at around 2.5 Hz, and in terms of frequency there was a difference from the frequency (approximately 1 Hz) of the predominant vibration in the Niigata Earthquake. On scrutiny of the fundamental vibration mode of the surface layer ground, the feature is that with layer No. 4 as a boundary, the layers above it behave as a single rigid body. Consequently, layer no. 4, which is a clay stratum, is subjected to extreme shear strains.

In the case of the Niigata Earthquake the difference in displacements at the top and bottom of layer No. 4 is estimated to have been 1 to 2 mm, and since the thickness of layer No. 4 is only about 20 cm, shear strain would have reached an order of 10^{-2}. Therefore, when it is considered that the propagation speed of S wave in cohesive soil is greatly changed by strain, it can be seen that the strain of this clay stratum will greatly affect the dynamic characteristics of the ground. Accordingly, it can be surmised that the influence of this clay stratum on dynamic properties, or earthquake motion at the surface layer, is governed by the nature of the earthquake at the basal rock.

It will be necessary to take this into consideration

when examining stability and the characteristics of earthquake motion at rocky ground.

Acknowledgements

In closing, the authors wish to express their sincerest gratitude to Mr. Katsuyuki Kato, Institute of Industrial Science, University of Tokyo, who mainly has carried out the earthquake observations on site, and to the gentlemen of Tokyo Electric Power Company, Inc. for their kind offices in making possible the earthquake observations on company property.

References

[1] S. Okamoto: Introduction to Earthquake Engineering, University of Tokyo Press, 1973.

[2] K. Kanai et al.: Comparative Studies of Earthquake Motions on the Ground and Underground (Multiple Reflection Problem), Bull. of Earthquake Research Institute, University of Tokyo, Vol. 37, pp. 53-87, 1959.

[3] K. Aki et al.: Spectral Study of Near Earthquake Waves (1), Bull. of Earthquake Research Institute, University of Tokyo, Vol. 36, pp. 71-98, 1958.

Table- 1 Geology and Seismometers

NOTE : W.G ; WEATHERED GREEN TUFF
C.G ; CLAYED GREEN TUFF

GEOLOGY				LOCATION OF SEISMOMETERS			
		NOTE		BORING HOLE		VERTICAL SHAFT	
GEOLOGY	DEPTH (M)	DEPTH(M)		DEPTH(M)	SIGN	DEPTH(M)	SIGN
ALLUVIAL DEPOSITE	0	0				0	ACC.NO.1 DIS.NO.1
COARSE GRAINED GREEN TUFF	7.9	10.90		9.0	NO.1		
		11.05	W.G				
		11.40					
		11.60	W.G	14.0	NO.2		
		15.70	C.G	16.5	NO.3	17.2	ACC.NO.2
		16.0					
		22.15					
		22.60	W.G				
		36.0		35.0	NO.4	34.2	ACC.NO.3
		36.2	C.G				
COARSE GRAINED G.T FINE GRAINED G.T SLATY TUFF	42.25			42.0	NO.5		
		47.0					
		47.1	C.G				
				50.0	NO.6	51.2	ACC.NO.4
COARSE GRAINED GREEN TUFF	57.50			58.0	NO.7		
				67.0	NO.8	67.2	ACC.NO.5 DIS.NO.2

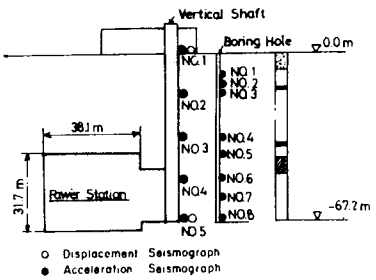

Fig. 1 Power Station and Location of Seismometers

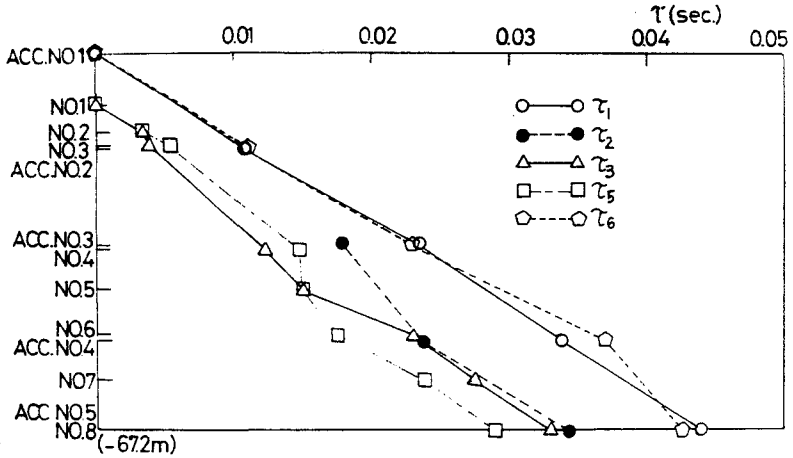

Fig. 2 Relation between Time lag and Depth of Accelerometers(Earthquake:June,17,1973)

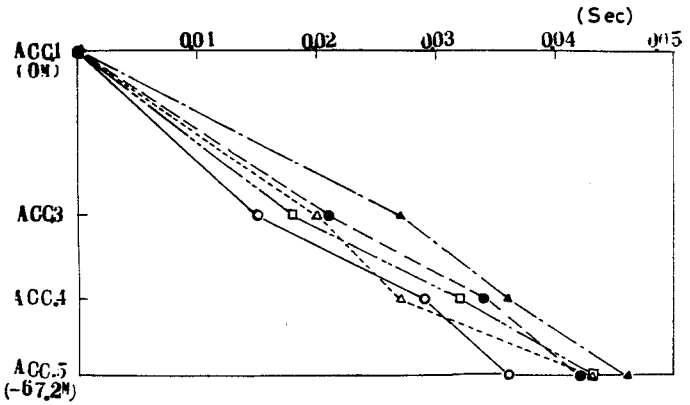

Fig. 4 Relation between Time lag and Depth of Accelerometers(Earthquake:Nov.,12,1964)

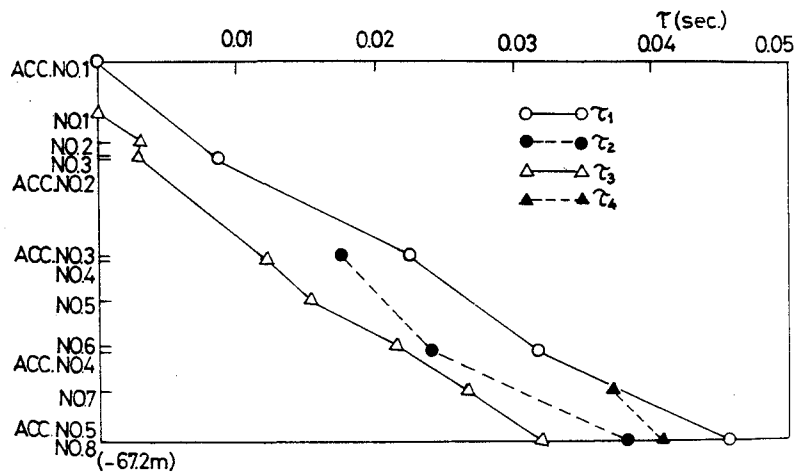

Fig. 3 Relation between Time lag and Depth of Accelerometers(Earthquake:June,13,1971)

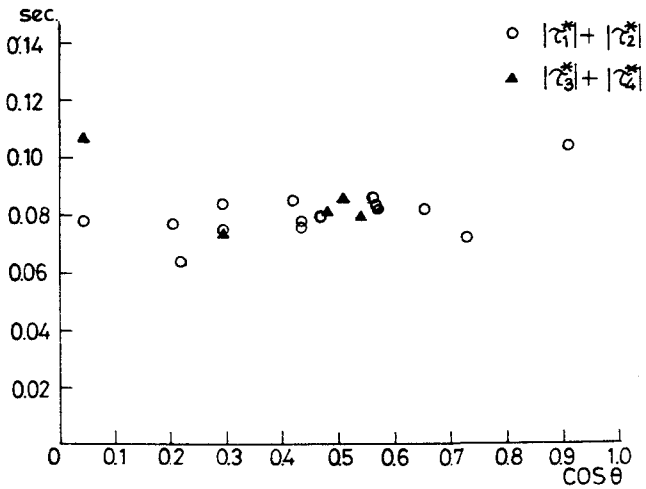

Fig. 5 Relation of Time lag to Angle Direction of the Hypocenter between Vertical Direction

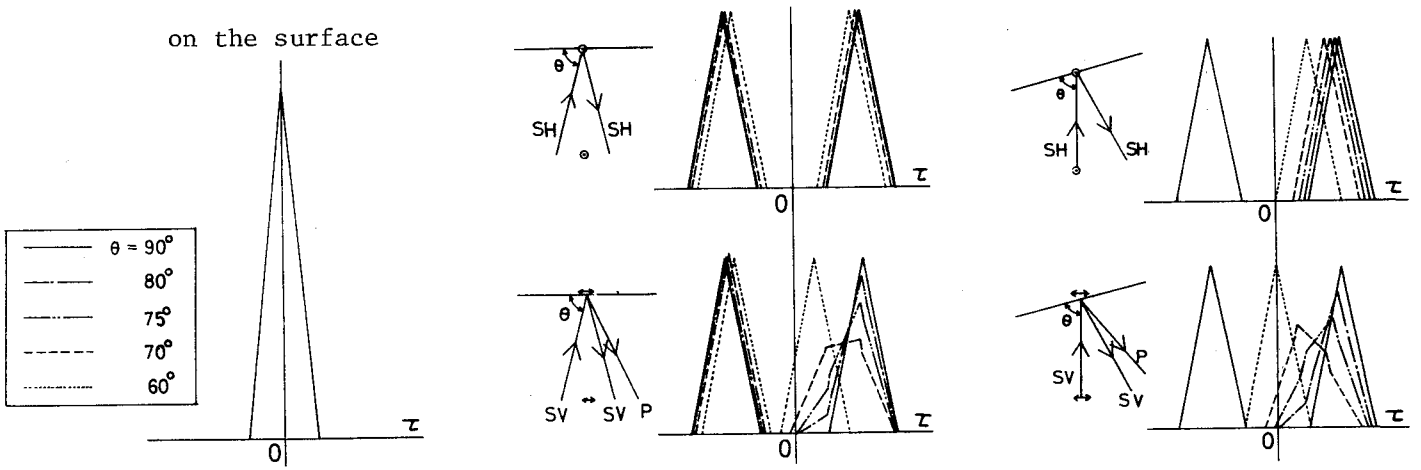

Fig. 6 Correlograms of Incident Wave and Reflected wave at the Depth to Wave on the Surface

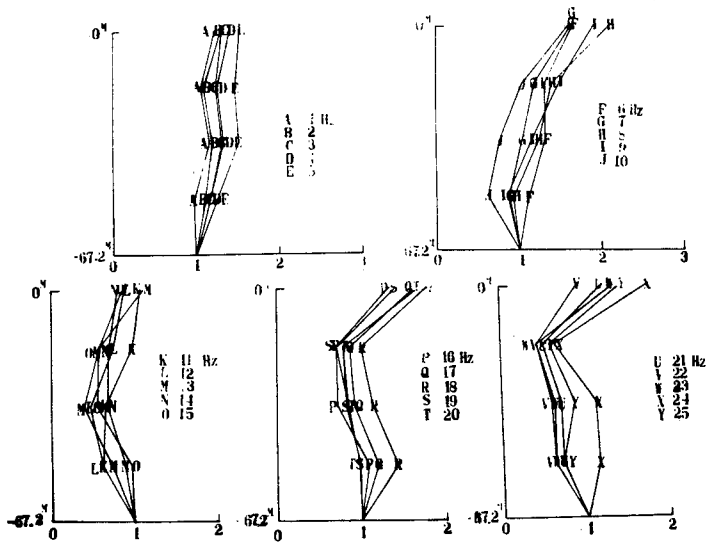

Fig. 7 Acceleration along the Depth

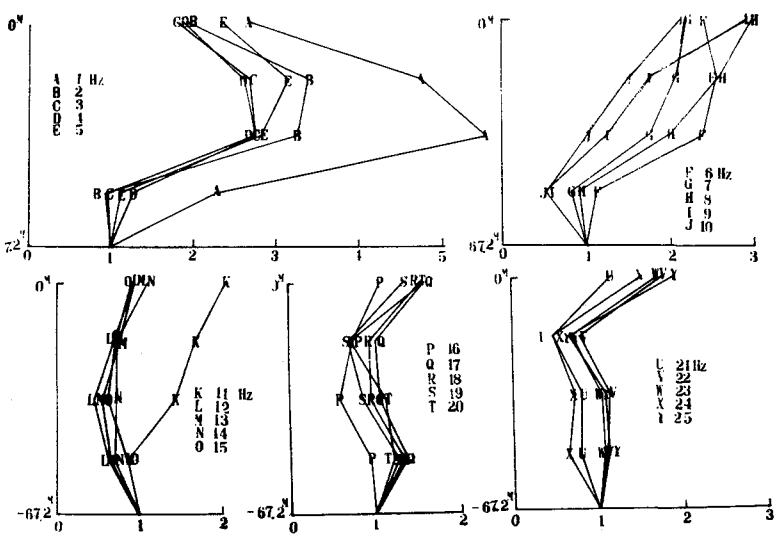

Fig. 8 Acceleration along the Depth

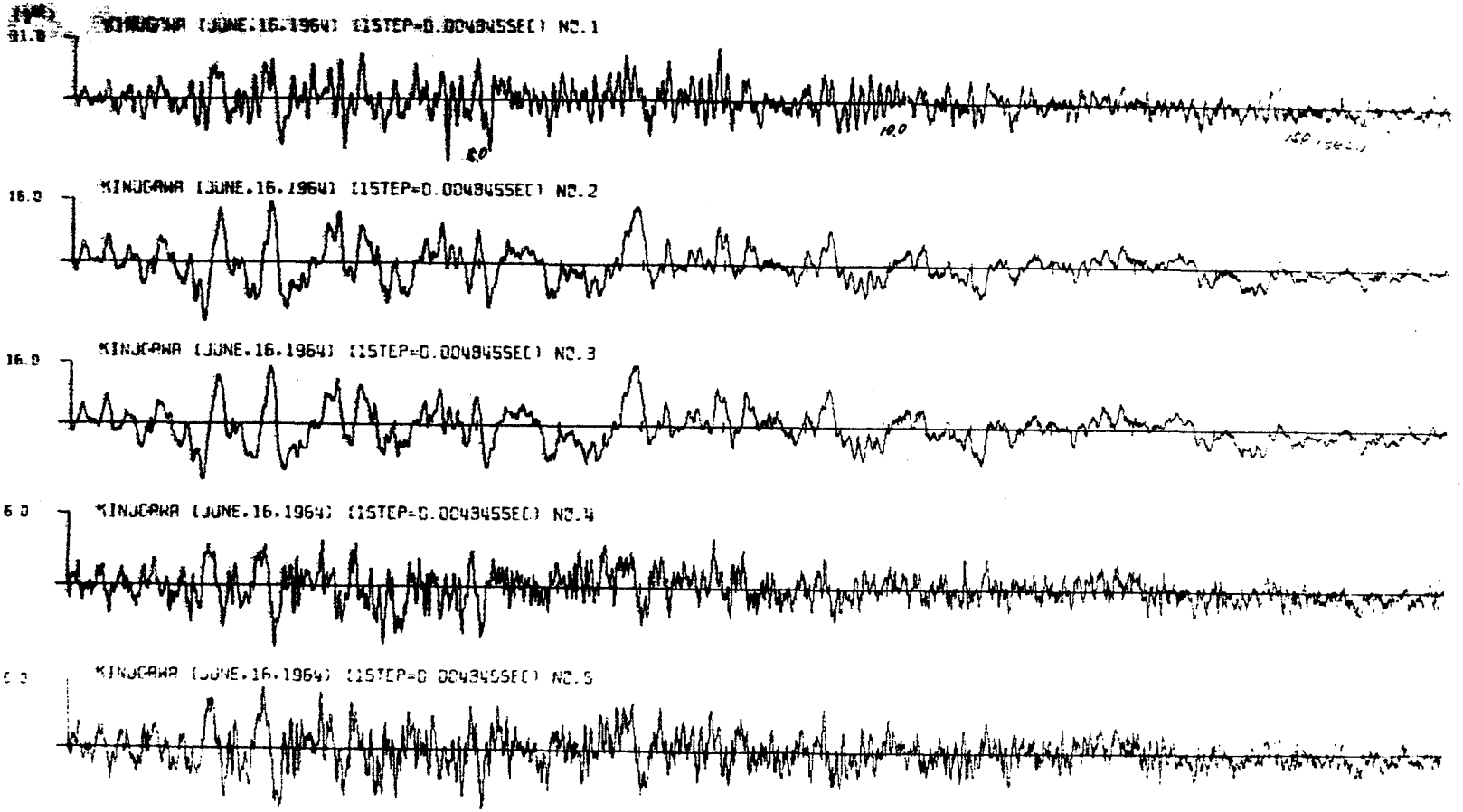

Fig. 9 Earthquake Records at Vertical Shaft (June,16,1964)

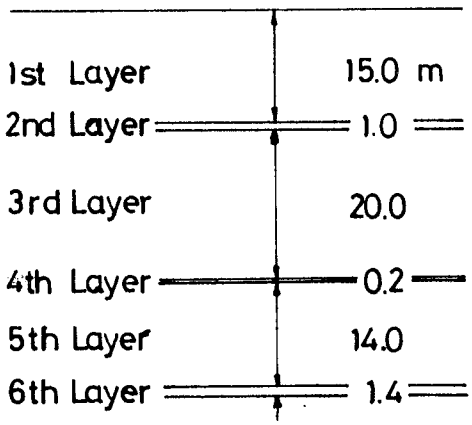

Fig.10 Surface Ground Model for Analysis

Table- 2 Physical Properties of Surface Ground

CASE	velocity of S-wave in m/sec.						natural frequency in Hz	
	v_1	v_2	v_3	v_4	v_5	v_6	f_1	f_2
1	1700	200	1700	100	1700	500	3.910	10.072
2		100		100			2.989	6.762
3		100		50			2.211	5.383
4		100		25			1.268	4.915
5		50		100			1.738	5.885
6		25		100			0.901	5.693
7		50		50			1.590	3.786
8		25		25			0.808	1.958
9		50		25			1.150	2.743
10		200		25			1.310	9.298
11		25		50			0.883	3.420
12		200		50			2.444	9.514
13	1700	200	1700	100	1700	1000	4.041	10.252
14		25		100			1.232	5.963
15		25		25			0.808	1.963
16		200		25			1.314	9.299
17		25		50			0.883	3.465
18		200		50			2.474	9.532
19	1000	100	1700	25	1700	1000	1.273	4.860
20	500	100	1700	25	1700	1000	1.269	4.612
21		50		25			1.148	2.712

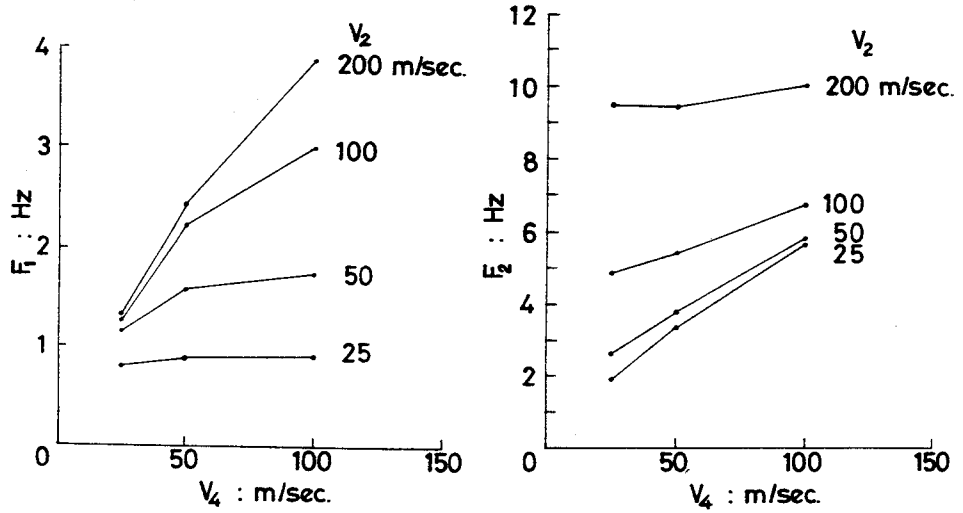

Fig.11 Natural Frequency and Velocity of S wave in 4th Layer

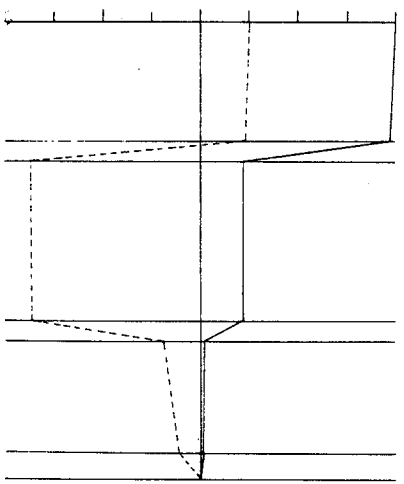

Fig.12 Natural Model in Case No.2

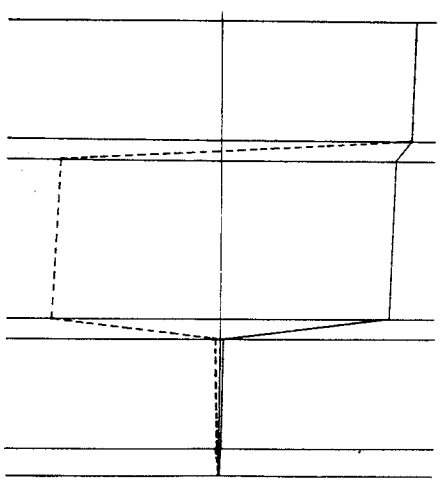

Fig.13 Natural Model in Case No.4

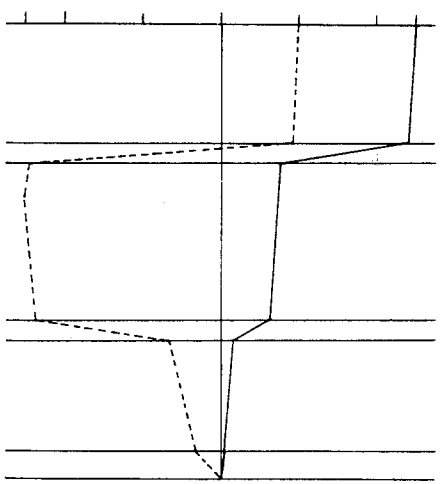

Fig.14 Natural Model in Case No.8

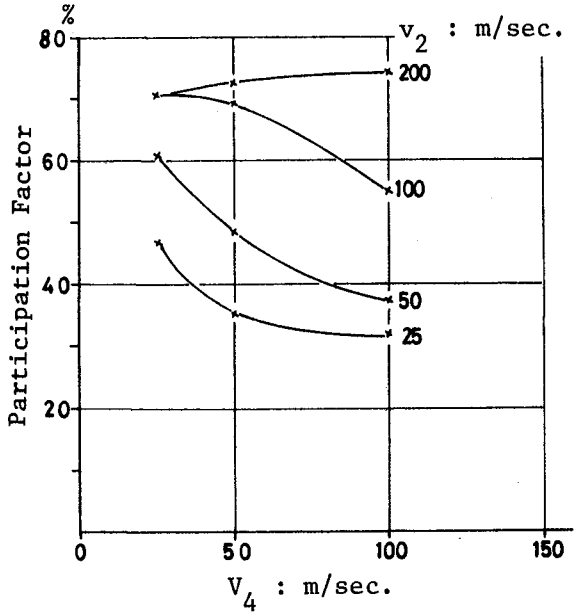

Fig.15 Participation Factor of Fundamental Vibration

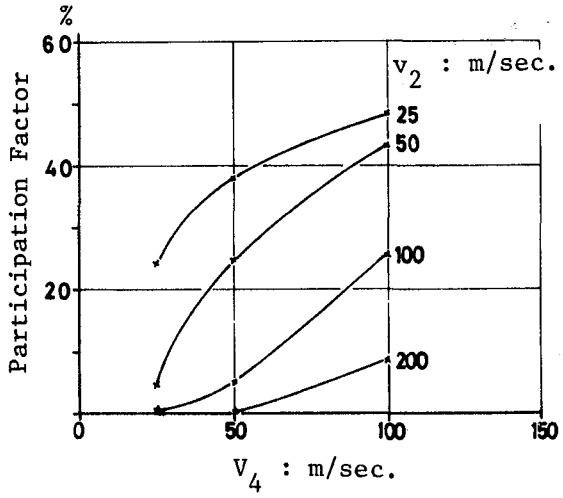

Fig.16 Participation Factor of 2nd order Vibration

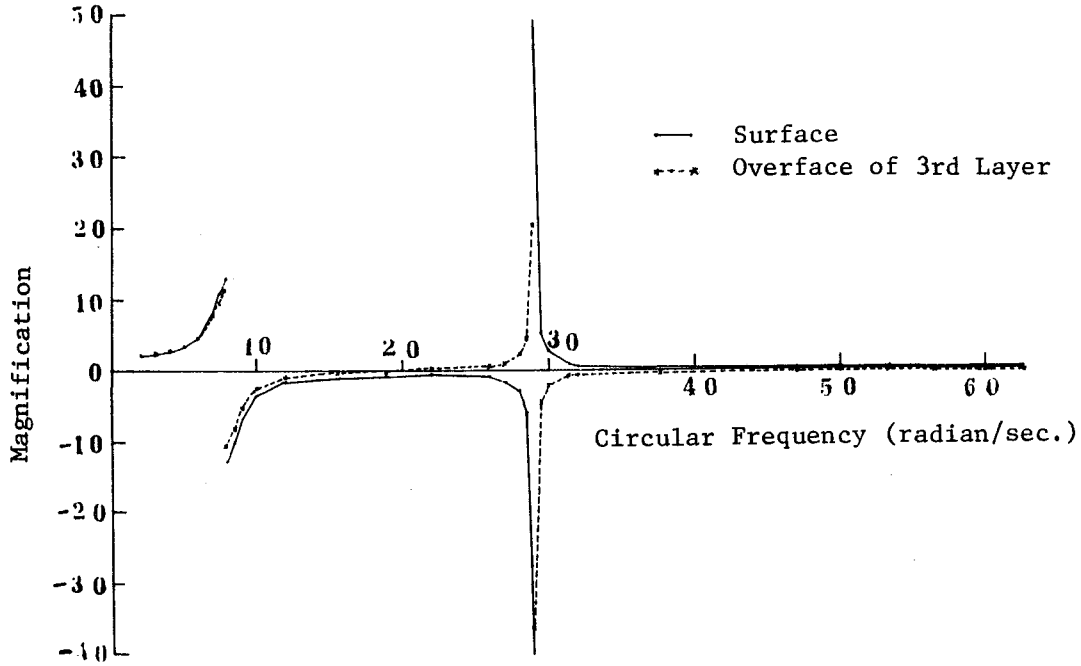

Fig.17 Response Curve to Unit Incident Wave in Case No.20

Table- 3 Earthquake List

Date and Time(J.S.T.)	M	H(km)	△(km)	max.Acc.(gal)	max.Disp.(μ)
1964. 2. 5, 20h31m	6.0	40	130	4.23	51.2
3.25, 11h45m	5.3	40	133	2.50	29.6
4. 4, 10h45m	-	-	-	-	-
5.30, 23h32m	6.2	40	147	3.65	116.5
6.16, 13h32m	5.0	0	151	0.31	13.6
13h36m	5.4	0	182	1.92	11.1
13h54m	5.0	20	169	0.15	8.6
15h55m	6.1	0	206	0.38	24.7
6.19, 19h07m	5.5	0	206	-	-
11. 3, 11h06m	5.2	100	239	0.46	14.6
11.12, 22h58m	4.9	0	81	3.85	40.0
11.14, 14h57m	5.1	40	91	9.23	123.5
11.16, 8h28m	4.5	20	53	3.42	24.7
1965. 4. 6, 14h32m	5.5	60	88	44.62	335.8
9.18, 1h21m	6.7	40	166	7.74	246.9
1974. 5. 9, 8h34m	6.9	10	264	2.75	333.3
8. 4, 3h16m	5.8	50	92	-	-
1975. 3.30, 4h58m	5.4	70	81	12.61	236.4

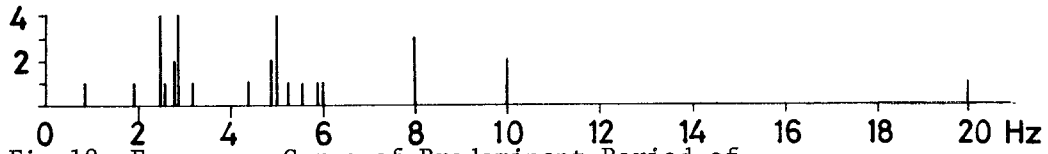

Fig.18 Frequency Curve of Predominant Period of Earthquake Listed in Table- 3

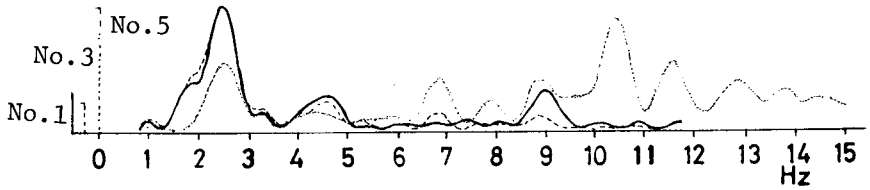

Fig.19 Power Spectra of Accelerogram(April,6,1965)

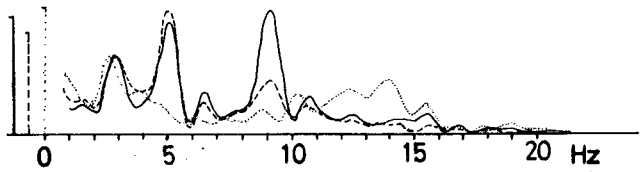

Fig.20 Power Spectra of Accelerogram(Sept.,18,1965)

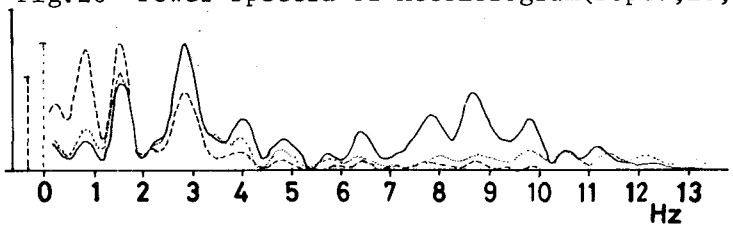

Fig.21 Power Spectra of Accelerogram(June,16,1964)

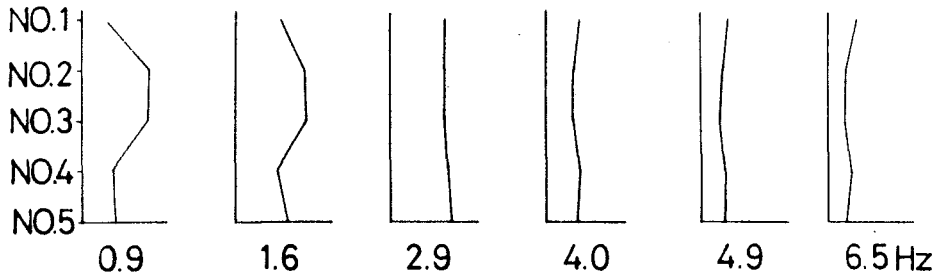

Fig.22 Acceleration along the Depth (June,16,1964)

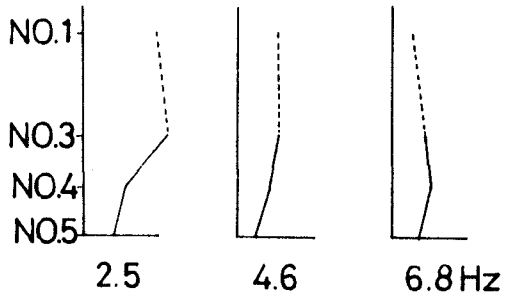

Fig.23 Acceleration along the Depth (April,6,1965)

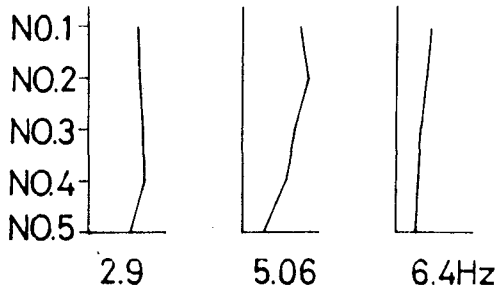

Fig.24 Acceleration along the Depth (Sept.,18,1965)

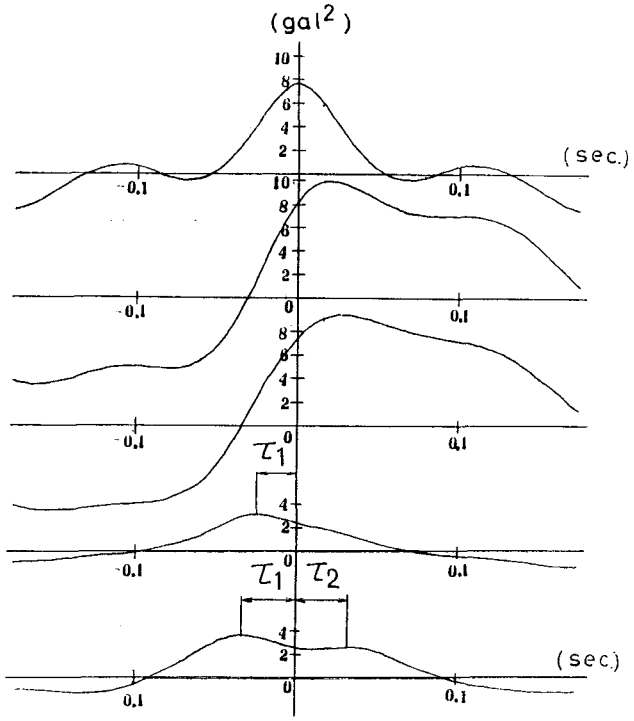

Fig.25 Correlograms of Records at each Depth to Surface Record